Curves, circles, and spheres

O. Gonzalez, J. H. Maddocks, and J. Smutny

ABSTRACT. The standard radius of curvature at a point $q(s)$ on a smooth curve can be defined as the limiting radius of circles through three points that all coalesce to $q(s)$. In the study of ideal knot shapes it has recently proven useful to consider a *global* radius of curvature of the curve at $q(s)$ defined as the *smallest* possible radius amongst all circles passing through this point and any two other points on the curve, coalescent or not. In particular, the minimum value of the global radius of curvature gives a convenient measure of curve thickness. Given the utility of the construction inherent to global curvature, it is also natural to consider variants of global radii of curvature defined in related ways. For example multi-point radius functions can be introduced as the radius of a sphere through four points on the curve, circles that are tangent at one point of the curve and intersect at another, etc. Then single argument, global radius of curvature functions can be constructed by minimizing over all but one argument. In this article we describe the interrelations between all possible global radius of curvature functions of this type, and show that there are two of particular interest. Properties of the divers global radius of curvature functions are illustrated with the simple examples of ellipses and helices, including certain critical helices that arise in the optimal shapes of compact filaments, in α-helical proteins, and in B-form DNA.

1. Introduction

Several applications within physics and biology lead to the following basic mathematical question: for a given curve $\boldsymbol{q}(s)$ in three dimensions, what is the distance from self-intersection? There are various optimal design problems that are associated with this distance; for example, amongst closed curves of a given knot type and prescribed length, what is the configuration, or ideal shape, that maximizes the distance from self-intersection [**4, 8, 12, 14, 18**]? Or what is the longest curve that can be placed in a given container, subject to a prescribed lower bound on the distance of closest approach [**15, 19**]? Similarly one could consider non-singular self-interaction energies on curves that take a closest-approach or related distance as argument [**3, 8**].

These rather natural and intuitive problems all depend on making the notion of distance from self-intersection precise. One way of doing this is to introduce the normal injectivity radius $\mathrm{Inj}[\boldsymbol{q}]$ for a curve $\boldsymbol{q}(s)$, see for example [**6**, p. 271], which can be described informally in the following way. At each point along the curve construct a circle in the normal plane with center at $\boldsymbol{q}(s)$, and for a given fixed radius consider the tubular envelope of these circles. For smooth curves and sufficiently small radii, the tubular surface so obtained will be smooth. However for sufficiently large radii the tubular surface will develop a singularity, either when circles from distinct points on the curve first touch, or when a crease develops with the tube radius equalling the local radius of curvature of the base curve at some point. Due to this geometrical construction, and following [**14**], the normal injectivity radius of a curve will here be called its thickness.

The above mathematical notion of thickness can be made entirely rigorous and, as the name suggests, it also can be used as a model for the actual thickness of physical filaments [**9**]. However, for the purposes of both numerical simulations and mathematical analysis the above geometrical definition suffers from the fact that it is implicit. In contrast, in [**8**] it was shown that the thickness of smooth, closed curves could be characterized explicitly as

$$(1.1) \qquad\qquad \mathrm{Inj}[\boldsymbol{q}] = \inf_{s,t,\sigma} \mathsf{ppp}(s,t,\sigma)$$

where the infimum is taken over all distinct points on the curve, and the function $\mathsf{ppp}(s,t,\sigma)$ is the radius of the circle through the points $\boldsymbol{q}(s)$, $\boldsymbol{q}(t)$ and $\boldsymbol{q}(\sigma)$. (The reciprocal of the function $\mathsf{ppp}(s,t,\sigma)$ is sometimes called the Menger curvature of the three points [**2**, p. 75].) In particular, the thickness of a curve can be defined as the infimum of a three-point distance function, namely the radius of a circle through three points on the curve. The analogous construction for the usual two-point Euclidean distance function is patently insufficient for defining thickness, by dint of the fact that curve continuity and the limit $s \to t$ implies

$$(1.2) \qquad\qquad 0 \equiv \inf_{s,t} \mathsf{pp}(s,t),$$

where $\mathsf{pp}(s,t)$ is our notation for half of the usual Euclidean distance between $\boldsymbol{q}(s)$ and $\boldsymbol{q}(t)$.

Once the characterization (1.1) and its implications have been accepted as establishing the utility of the multi-point distance function $\mathsf{ppp}(s,t,\sigma)$ that is based upon the radius of a circle through points on a curve, Pandora's box is opened and many different further possibilities arise. For the sake of simplicity, in this article we shall give full consideration only to generic sets of points (and coalescent limits thereof) on smooth curves, so that sets of three points are assumed non-collinear, sets of four points non-coplanar, and so on. With this understanding, four distinct points on the curve define a unique sphere with a zeroth-order intersection at each of the four points, three distinct points define a unique circle with a zeroth-order contact at each of the three points, or a unique sphere with zeroth-order contact at two of the points and a first-order contact, or tangency, at the third, and so on. We introduce a mnemonic notation for the radii of the corresponding objects, e.g. $\mathsf{pppp}(s,t,\sigma,\tau)$ for the radius of the sphere with zeroth-order contacts at $\boldsymbol{q}(s)$, $\boldsymbol{q}(t)$, $\boldsymbol{q}(\sigma)$ and $\boldsymbol{q}(\tau)$ (where p stands for point), $\mathsf{ppp}(s,t,\sigma)$ for the radius of the circle with zeroth-order contacts at $\boldsymbol{q}(s)$, $\boldsymbol{q}(t)$ and $\boldsymbol{q}(\sigma)$ (as before), while $\mathsf{ptp}(s,t,\sigma)$ denotes the radius of the sphere with zeroth-order contacts at $\boldsymbol{q}(s)$ and $\boldsymbol{q}(\sigma)$, and

a first-order contact or tangency at $\boldsymbol{q}(t)$. No assumption is made on the ordering of the values taken by the arguments of these functions, so that we have trivial identities arising from permutations, such as $\mathsf{pppp}(s,t,\sigma,\tau) = \mathsf{pppp}(s,t,\tau,\sigma)$ and $\mathsf{ptp}(s,t,\sigma) = \mathsf{ppt}(s,\sigma,t)$. However, typically $\mathsf{ptp}(s,t,\sigma) \neq \mathsf{ppt}(s,t,\sigma) \neq \mathsf{tpp}(s,t,\sigma)$. We use c (for circle) as the mnemonic notation for second-order contact, so that $\mathsf{cp}(s,t)$ denotes the sphere with zeroth-order contact at $\boldsymbol{q}(t)$ and second-order contact at $\boldsymbol{q}(s)$. In other words, $\mathsf{cp}(s,t)$ is the radius of the unique sphere containing the point $\boldsymbol{q}(t)$ and the standard osculating circle of the curve at $\boldsymbol{q}(s)$. Finally, we retain the traditional notation $\rho(s)$ (rather than $\mathsf{c}(s)$) for the radius of the osculating circle at the point $\boldsymbol{q}(s)$, and we adopt $\rho_{\mathrm{os}}(s)$ for the radius of the osculating sphere, which has contact of order three at $\boldsymbol{q}(s)$ (see Section 3).

Table 1 summarizes all thirteen, distinct, multi-point distance functions which arise as radii of line segments, circles and spheres that are defined by various orders of contact to a given curve at one, two, three or four distinct points. The row in the table indicates whether it is the radius of a line segment, circle, or sphere (which may be interpreted as zero-, one- or two-dimensional spheres), while the column indicates the number of distinct arguments in the corresponding function. These functions are studied in Section 4 where various inequalities between entries in each column are derived. In particular, we find that while there is generally no ordering among the functions contained in any one block of the table, within one column a function appearing in a higher row is bounded above by any function appearing in a lower row. The only exceptions to this rule are the two functions cp and pc that are marked with asterisks; there are only partial orderings between these functions and those appearing above them.

	1	2	3	4
line	0	pp		
circle	ρ	pt tp	ppp	
sphere	ρ_{os}	cp* pc* tt	tpp ptp ppt	pppp

TABLE 1. All possible multi-point radius functions that are defined in terms of line segments, circles and spheres. Rows correspond to the type of object, while columns correspond to the number of arguments associated with each radius function. With the exception of the two asterisked functions, the following inequalities hold: within a given column, and when evaluated at the same arguments, any function appearing in a higher of the three rows is smaller than any function appearing in a lower row.

Our motivation for introducing the above functions is to consider potentially useful generalizations of the global radius of curvature function that was introduced in [8]. For reasons that will become apparent later, within the current article we will change from the notation ρ_G of [8] for the global radius of curvature function to the notation ρ_{ppp}. The central tenet of global radius of curvature is to start from a multi-point radius function such as $\mathsf{ppp}(s,t,\sigma)$, and to produce a nonlocally

defined, global radius of curvature function along the curve through minimization over all but the first of the multi-point arguments, thus

$$(1.3) \qquad \rho_{\mathsf{ppp}}(s) = \inf_{t,\sigma} \mathsf{ppp}(s, t, \sigma)$$

where the infimum is taken over all distinct points on the curve. The coalescent limit of $\boldsymbol{q}(\sigma), \boldsymbol{q}(t) \to \boldsymbol{q}(s)$ is one possible competitor in this minimization, so the classic local radius of curvature is an upper bound for the global radius of curvature. But in general the global radius of curvature can sample the curve non-locally, and is strictly smaller than the local radius of curvature (see Figure 1). Indeed, in Section 5 of this article we will demonstrate that the local radius of curvature $\rho(s)$ can equal the global radius of curvature $\rho_{\mathsf{ppp}}(s)$ only at extremal points of $\rho(s)$ (and that even this stringent necessary condition is by no means sufficient).
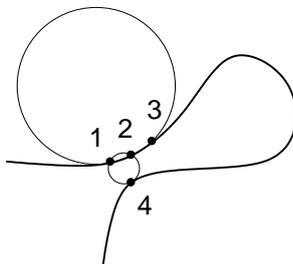

FIGURE 1. The radius of the circle through three neighboring points along a curve, such as 1, 2 and 3, approximates the local radius of curvature at the point 2. In contrast, a global radius of curvature at the point 2 contains information concerning non-local parts of the curve, e.g. the fact that there are rather small circles through the point 2 and two other points of the curve such as 1 and 4.

It may now be seen that each of the thirteen multi-point radius functions introduced in Table 1 generates a global radius of curvature function, analogous to (1.3), when it is minimized over all but its first argument. Of course the one-point functions of the first column remain unchanged, as there is no minimization to carry out. Moreover, by (1.2) we find that minimization of the two-point radius function pp yields the zero function. Thus, there remain twelve nontrivial global radius of curvature functions as shown in Table 2. We denote all of these functions by ρ with the subscript that is inherited from the mnemonic name introduced in Table 1.

The global radius of curvature functions introduced in Table 2 are studied in Section 5. In addition to the column inequalities carried over from Table 1, there are now also row inequalities. Specifically, (and for simplicity again ignoring the two asterisked functions) it can be shown that along each row, any function dominates any other function appearing in a column to its right. This fact follows from a simple comparison on the set of competitors involved in the minimization that leads to the global curvature function. The more surprising conclusion is that, for curves that are either closed or infinite, but are otherwise arbitrary, amongst the row and column inequalities, there are in fact several identities. (Possible interactions with end-points complicates matters, but for closed or infinite curves there are no end-points.) As a consequence, amongst the twelve non-trivial radius of curvature

	0	1	2	3
line	0	$\rho_{\mathsf{pp}} = 0$		
circle	ρ	ρ_{pt} ρ_{tp}	ρ_{ppp}	
sphere	ρ_{os}	$\rho_{\mathsf{cp}}{}^{\star}$ $\rho_{\mathsf{pc}}{}^{\star}$ ρ_{tt}	ρ_{tpp} ρ_{ptp} ρ_{ppt}	ρ_{pppp}

TABLE 2. Global radius of curvature functions. Each function of a single variable is defined by minimization of the multi-point functions of Table 1 over all but their first argument. Rows correspond to the type of object, while columns correspond to the number of minimizations associated with the function. Only five of the twelve functions are distinct on smooth curves that are closed or infinite.

functions appearing in Table 2, there are only five independent ones, for example ρ, ρ_{os}, ρ_{pt}, ρ_{pc}, and ρ_{tt}.

We argue that the two most interesting global radius of curvature functions are ρ_{pt} (as considered in [**8**]) and ρ_{tt}. For example, in Section 6 we demonstrate that the thickness, or normal injectivity radius, of any closed or infinite curve equals the (common) minimal value of ρ_{pt} and ρ_{tt} along the curve. It is noteworthy that numerical evaluation of ρ_{pt} or ρ_{tt} at a given point on a curve involves only a one-dimensional minimization (because they each appear in the second columns of Tables 1 and 2). In contrast, evaluation of a function such as ρ_{ppp} would involve a two-dimensional search, which is *a priori* a much more intensive computation.

In Section 7 we close the presentation with illustrations of various of the multi-point radius and global radius of curvature functions in the particular cases of ellipses, and helical structures.

Finally it should be noted that while for simplicity we consider only smooth curves in this article, many of the results that we present can be extended to curves that are not smooth. For example, a uniform lower bound on a suitable multi-point radius function has been used to establish regularity of *a priori* non-smooth curves [**4, 7, 9, 17**].

2. Preliminaries

By a *curve* Γ we mean a continuous three-dimensional vector function $\boldsymbol{q}(s)$ of a real variable s. We consider curves Γ that are either (a) *finite* by which we mean the parameter s takes values in a closed interval $[0, L]$ with the set $\boldsymbol{q}(s)$ being bounded, or (b) *infinite* in the sense that s takes values in the open interval $(-\infty, \infty)$ and $|\boldsymbol{q}(s)| \to \infty$ as $|s| \to \infty$. (Of course, these two cases are not exhaustive, but they suffice for our interests.)

A curve Γ is *smooth* if the function $\boldsymbol{q}(s)$ is continuously differentiable to any order and if the tangent vector $\boldsymbol{q}'(s)$ is nonzero for all s. In the smooth case we interpret s as the arclength parameter. We denote the standard local curvature and torsion of Γ at $\boldsymbol{q}(s)$ by $\kappa(s)$ and $\tau(s)$, and we denote the local Frenet frame of tangent, principal normal and binormal by $\{\boldsymbol{t}(s), \boldsymbol{n}(s), \boldsymbol{b}(s)\}$ wherever it is defined. Throughout, all curves will be assumed to be smooth and finite in the sense of possibility (a) above, unless explicit mention to the contrary is made. We shall

consider the infimum of various functionals defined on both finite and infinite curves. For simplicity of exposition we shall implicitly assume throughout that the infima are attained at finite points $q(s)$ on the curve.

A curve Γ is *closed* if $q(L) = q(0)$, in which case we interpret the parameter s modulo L. Moreover, if Γ is smoothly closed, the derivatives of all orders of $q(s)$ agree at $s = 0$ and $s = L$. Finally, a curve Γ is *simple* if it has no self-intersections, that is, $q(s_1) = q(s_2)$ only when $s_1 = s_2$.

3. Local circles and spheres

The local behavior of a curve Γ at a point $q(s)$ can be described in terms of various osculating or tangent objects: the osculating line $\mathcal{L}(s)$, plane $\mathcal{P}(s)$, circle $\mathcal{C}(s)$, sphere $\mathcal{S}(s)$ and circumsphere $\mathcal{S}^c(s)$. All but the last are standard objects in the differential geometry of curves.

3.1. Definitions. $\mathcal{L}(s)$ is the line through $q(s)$ spanned by $t(s)$. When $\kappa \neq 0$, $\mathcal{P}(s)$ is the plane through $q(s)$ spanned by the tangent and principal normal $\{t(s), n(s)\}$, and $\mathcal{C}(s)$ is the circle contained in $\mathcal{P}(s)$ with center

$$(3.1) \qquad c(s) = q(s) + \rho(s)n(s),$$

and radius

$$(3.2) \qquad \rho(s) = \frac{1}{\kappa(s)},$$

i.e. the standard local radius of curvature. When both $\kappa \neq 0$ and $\tau \neq 0$, the osculating sphere $\mathcal{S}(s)$ [**20**, p. 25], which is the sphere through four coalescent points, has center

$$(3.3) \qquad c_{\mathrm{os}}(s) = q(s) + \rho(s)n(s) + \frac{\rho'(s)}{\tau(s)}b(s)$$

and radius

$$(3.4) \qquad \rho_{\mathrm{os}}(s) = \sqrt{\rho^2(s) + \left(\frac{\rho'(s)}{\tau(s)}\right)^2}.$$

We will also make use of another locally-defined sphere, which we call the *osculating circumsphere* and denote $\mathcal{S}^c(s)$, that is defined to be the unique sphere of radius $\rho(s)$ that contains $\mathcal{C}(s)$ as a great circle. The osculating circle is always contained in the intersection of the osculating sphere and osculating circumsphere, and, in general, it is all of the intersection because (3.4) reveals that typically $\rho_{os} > \rho$.

Remarks 3.1

1. The objects $\mathcal{L}(s)$, $\mathcal{P}(s)$, $\mathcal{C}(s)$ and $\mathcal{S}(s)$ may be defined in terms of their contact order with Γ [**10**, p. 26, 72], [**20**, p. 23]. For example, $\mathcal{L}(s)$ is the unique line that has a contact order of at least one with Γ at $q(s)$. When $\kappa(s) \neq 0$, $\mathcal{P}(s)$ is the unique plane that has a contact order of at least two, and so on.
2. When $\kappa(s) = 0$, we set $\rho(s) = \infty$, and identify the osculating circle with the osculating line. The osculating plane, sphere and circumsphere may or may not be uniquely defined depending on the behavior of κ and τ near s. In all cases it is consistent to set $\rho_{\mathrm{os}}(s) = \infty$ since any limit of (3.4) must be infinite.

3. When $\kappa(s) \neq 0$, but $\tau(s) = 0$, the osculating sphere again may or may not be uniquely defined depending on the limiting behavior of κ and τ near s. Following the contact-order arguments in [10, p. 72] we set

$$\mathcal{S}(s) = \begin{cases} \mathcal{P}(s), & \text{if } \lim_{\sigma \to s} \rho'(\sigma)/\tau(\sigma) \text{ is infinite} \\ \lim_{\sigma \to s} \mathcal{S}(\sigma), & \text{if } \lim_{\sigma \to s} \rho'(\sigma)/\tau(\sigma) \text{ is finite} \\ \mathcal{S}^c(s), & \text{if } \lim_{\sigma \to s} \rho'(\sigma)/\tau(\sigma) \text{ is undefined.} \end{cases}$$

The problematic last case occurs, for example, when Γ is itself a circle. It could be handled differently; for example the osculating sphere of a circle is explicitly left undefined in [10, p. 74].
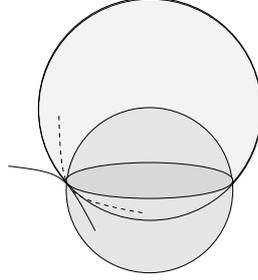

FIGURE 2. Geometrical interpretation of the Taylor expansions (3.5) and (3.6). The spheres $\mathcal{S}$ and $\mathcal{S}^c$ intersect on the osculating circle $\mathcal{C}$, and thereby define four spherical quadrants, corresponding to the intersections of the interiors and exteriors of the two spheres. Locally and generically, a curve lies either outside (solid curve) or inside (dashed curve) the (larger) osculating sphere $\mathcal{S}$, whereas it crosses the (smaller) osculating circumsphere $\mathcal{S}^c$, i.e. the curve passes between the four spherical quadrants in a highly constrained way.

3.2. Relationships, properties. At each point $\boldsymbol{q}(s)$ on a curve Γ the osculating line $\mathcal{L}(s)$, plane $\mathcal{P}(s)$, circle $\mathcal{C}(s)$, sphere $\mathcal{S}(s)$ and circumsphere $\mathcal{S}^c(s)$ enjoy the following relationships:

$$\begin{array}{rcll} \mathcal{C} & = & \mathcal{P} \cap \mathcal{S} & (\kappa \neq 0, \quad \tau \neq 0) \\ \mathcal{C} & = & \mathcal{L} & (\kappa = 0) \\ \rho & \leq & \rho_{\text{os}} & (\text{any } \kappa, \tau). \end{array}$$

Moreover, while Γ is tangent to both the osculating sphere $\mathcal{S}$ and circumsphere $\mathcal{S}^c$, when $\kappa \neq 0$ and $\tau \neq 0$ we find that, generically and locally, Γ pierces or crosses $\mathcal{S}^c$, but lies on one side or the other of the sphere $\mathcal{S}$, as illustrated in Figure 2. For $\mathcal{S}^c(s)$ this conclusion follows from the h^3 coefficient in the Taylor expansion

$$(3.5) \qquad |\boldsymbol{q}(s+h) - \boldsymbol{c}(s)|^2 = \frac{1}{\kappa^2} - \left(\frac{\kappa'}{3\kappa}\right)h^3 + \left(\frac{\tau^2}{12} - \frac{\kappa''}{12\kappa}\right)h^4 + O(h^5),$$

while the result for $\mathcal{S}(s)$ follows from the h^4 coefficient in the Taylor expansion

$$
\begin{aligned}
(3.6) \qquad |\boldsymbol{q}(s+h) - \boldsymbol{c}_{\mathrm{os}}(s)|^2 &= \frac{1}{\kappa^2} + \frac{\kappa'^2}{\tau^2\kappa^4} \\
&+ \left(\frac{\tau^2}{12} - \frac{\kappa''}{12\kappa} + \frac{\kappa'^2}{6\kappa^2} + \frac{\kappa'\tau'}{12\tau\kappa} \right) h^4 + O(h^5).
\end{aligned}
$$

4. Global circles and spheres

Just as the local behavior of a curve can be described in terms of local osculating lines, circles and spheres, aspects of the global behavior of a curve can be described by analogous multi-point objects: two-point line segments $\mathcal{L}(s,t)$, three-point circles $\mathcal{C}(s,t,\sigma)$ and four-point spheres $\mathcal{S}(s,t,\sigma,\tau)$. Here we study these objects and use them to introduce various generalized global radius of curvature functions for curves.

4.1. Definitions. Let Γ be a simple curve. Then for any two distinct points $\boldsymbol{q}(s)$ and $\boldsymbol{q}(t)$ we define $\mathcal{L}(s,t)$ to be the unique line segment between them with half-length

$$
(4.1) \qquad \mathsf{pp}(s,t) = \frac{1}{2}|\boldsymbol{q}(s) - \boldsymbol{q}(t)|.
$$

For any three non-collinear points $\boldsymbol{q}(s)$, $\boldsymbol{q}(t)$ and $\boldsymbol{q}(\sigma)$ we define $\mathcal{C}(s,t,\sigma)$ to be the unique circle (the circumcircle) that contains them, with radius (the circumradius) given by any of the classic formulæ [**5**, p. 13]:

$$
(4.2) \qquad \mathsf{ppp}(s,t,\sigma) = \frac{2\mathsf{pp}(s,t)\mathsf{pp}(s,\sigma)\mathsf{pp}(t,\sigma)}{\mathcal{A}(s,t,\sigma)}
$$

where $\mathcal{A}(s,t,\sigma)$ is the area of the triangle with vertices $\boldsymbol{q}(s)$, $\boldsymbol{q}(t)$ and $\boldsymbol{q}(\sigma)$, or

$$
(4.3) \qquad \mathsf{ppp}(s,t,\sigma) = \frac{\mathsf{pp}(s,\sigma)}{|\sin\theta_{st\sigma}|} = \frac{\mathsf{pp}(t,s)}{|\sin\theta_{t\sigma s}|} = \frac{\mathsf{pp}(\sigma,t)}{|\sin\theta_{\sigma st}|}
$$

where $\theta_{st\sigma}$ is the angle between the edge vectors $\boldsymbol{q}(s) - \boldsymbol{q}(t)$ and $\boldsymbol{q}(\sigma) - \boldsymbol{q}(t)$, and so on. The three forms in (4.3) all coincide by the Sine Rule of elementary geometry. (Note that typically these formulæ are written in terms of edge lengths, but for us the factor of one half in the definition (4.1) of pp is convenient, so we work with half of the edge lengths.) The circle radius can also be written as a ratio involving a Cayley-Menger determinant [**1**, p. 241], namely

$$
(4.4) \qquad \mathsf{ppp}^2(s,t,\sigma) = -2\frac{\Delta_{(3)}}{\Gamma_{(3)}},
$$

where

$$
(4.5) \qquad \Delta_{(3)} = \begin{vmatrix} 0 & \mathsf{pp}^2(s,t) & \mathsf{pp}^2(s,\sigma) \\ \mathsf{pp}^2(s,t) & 0 & \mathsf{pp}^2(t,\sigma) \\ \mathsf{pp}^2(s,\sigma) & \mathsf{pp}^2(t,\sigma) & 0 \end{vmatrix},
$$

and

$$
(4.6) \qquad \Gamma_{(3)} = \begin{vmatrix} 0 & \mathsf{pp}^2(s,t) & \mathsf{pp}^2(s,\sigma) & 1 \\ \mathsf{pp}^2(s,t) & 0 & \mathsf{pp}^2(t,\sigma) & 1 \\ \mathsf{pp}^2(s,\sigma) & \mathsf{pp}^2(t,\sigma) & 0 & 1 \\ 1 & 1 & 1 & 0 \end{vmatrix}.
$$

It is the Cayley-Menger form of the radius formula that generalizes to spheres. For any four non-coplanar points $q(s)$, $q(t)$, $q(\sigma)$ and $q(\tau)$ we define $\mathcal{S}(s,t,\sigma,\tau)$ to be the unique sphere that contains them. The radius of this sphere, denoted $\mathsf{pppp}(s,t,\sigma,\tau)$, satisfies

$$(4.7) \qquad \mathsf{pppp}^2(s,t,\sigma,\tau) = -2\frac{\Delta_{(4)}}{\Gamma_{(4)}},$$

where the 4×4 determinant $\Delta_{(4)}$ and 5×5 determinant $\Gamma_{(4)}$ are the natural generalizations of (4.5) and (4.6) written in terms of the six edge half-lengths.

Remarks 4.1

1. At any distinct pair, non-collinear triple, or non-coplanar quadruple of points, the functions pp, ppp and pppp are, respectively, continuous and symmetric in their arguments.
2. When (s,t,σ) are distinct but collinear, we set $\mathsf{ppp}(s,t,\sigma) = \infty$. Similarly, when (s,t,σ,τ) are distinct but coplanar, we set $\mathsf{pppp}(s,t,\sigma,\tau) = \infty$, unless these points are co-circular in which case we set $\mathsf{pppp}(s,t,\sigma,\tau) = \mathsf{ppp}(s,t,\sigma)$.
3. The sphere $\mathcal{S}(s,t,\sigma,\tau)$ enjoys several equivalent geometric characterizations at any quadruple of non-coplanar points. For example, it is the unique sphere defined by the point $q(s)$ and the circle $\mathcal{C}(t,\sigma,\tau)$, but is also the unique sphere defined by the point $q(t)$ and the circle $\mathcal{C}(s,\sigma,\tau)$ and so on. These equivalent characterizations will be exploited below.

4.2. Coalescent functions. Various radius functions can be derived from ppp and pppp by considering (generic) coalescent limits along the curve Γ. For example, from the three-point function we obtain

$$\mathsf{ppp}(s,t,\sigma) \overset{\sigma \to t}{\to} \mathsf{pt}(s,t) \overset{t \to s}{\to} \rho(s), \quad (s,t,\sigma \quad \text{non-collinear}).$$

Here $\mathsf{pt}(s,t)$ is the radius of the unique circle that passes through $q(s)$ and is tangent to Γ at $q(t)$. We denote this circle by $\mathcal{C}(s,t,t)$ and note that it is actually the limit of $\mathcal{C}(s,t,\sigma)$ as $q(\sigma) \to q(t)$ along Γ. As before, $\rho(s)$ is the radius of the standard osculating circle $\mathcal{C}(s)$ at $q(s)$. Thus we recover the classic result that the osculating circle may be interpreted as $\mathcal{C}(s,s,s)$, the limit of $\mathcal{C}(s,t,\sigma)$ as $q(\sigma), q(t) \to q(s)$ along Γ.

By changing the order of the first limit we obtain a slightly different result, namely

$$\mathsf{ppp}(s,t,\sigma) \overset{t \to s}{\to} \mathsf{tp}(s,\sigma) \overset{\sigma \to s}{\to} \rho(s), \quad (s,t,\sigma \quad \text{non-collinear}).$$

Here $\mathsf{tp}(s,t)$ is the radius of the unique circle $\mathcal{C}(s,s,t)$ that passes through $q(t)$ and is tangent to Γ at $q(s)$. In particular, we have $\mathsf{tp}(s,t) = \mathsf{pt}(t,s)$, but $\mathsf{tp}(s,t) \neq \mathsf{tp}(t,s) = \mathsf{pt}(s,t)$, because, in general, both of the two-point circular radius functions are non-symmetric in their arguments.

Analogous limits may also be considered for the four-point function pppp. For example,

$$\mathsf{pppp}(s,t,\sigma,\tau) \overset{\tau \to \sigma}{\to} \mathsf{ppt}(s,t,\sigma) \overset{\sigma \to t}{\to} \mathsf{pc}(s,t) \overset{t \to s}{\to} \rho_{\mathrm{os}}(s), \quad (s,t,\sigma,\tau \quad \text{non-coplanar}).$$

Here $\mathsf{ppt}(s,t,\sigma)$ is the radius of the unique sphere defined by the point $q(s)$ and the circle $\mathcal{C}(t,\sigma,\sigma)$. Similarly, $\mathsf{pc}(s,t)$ is the radius of the unique sphere defined by

the point $\boldsymbol{q}(s)$ and the osculating circle $\mathcal{C}(t,t,t)$. As before, $\rho_{\mathrm{os}}(s)$ is the radius of the osculating sphere at $\boldsymbol{q}(s)$.

By changing the order of the limits we obtain various different three-point functions analogous to ppt, and various different two-point functions analogous to pc. The different functions may be represented in the following way:

$$\mathsf{pppp} \overset{4\mathrm{pt}\to3\mathrm{pt}}{\to} \left\{ \begin{array}{c} \mathsf{ppt} \\ \mathsf{ptp} \\ \mathsf{tpp} \end{array} \right\} \overset{3\mathrm{pt}\to2\mathrm{pt}}{\to} \left\{ \begin{array}{c} \mathsf{pc} \\ \mathsf{cp} \\ \mathsf{tt} \end{array} \right\} \overset{2\mathrm{pt}\to1\mathrm{pt}}{\to} \rho_{\mathrm{os}}.$$

For example, $\mathsf{ptp}(s,t,\sigma)$ is the radius of the unique sphere defined by the point $\boldsymbol{q}(s)$ and the circle $\mathcal{C}(t,t,\sigma)$, or, equivalently, defined by the point $\boldsymbol{q}(\sigma)$ and the circle $\mathcal{C}(s,t,t)$. The two-point function $\mathsf{tt}(s,t)$ is the radius of the unique sphere defined by the two circles $\mathcal{C}(s,s,t)$ and $\mathcal{C}(s,t,t)$. In particular, $\mathsf{tt}(s,t)$ is the radius of the sphere that is tangent to $\varGamma$ at both $\boldsymbol{q}(s)$ and $\boldsymbol{q}(t)$.

4.3. Explicit formulæ. Explicit formulæ for the coalescent limit functions are available whenever the remaining arguments are in generic position. For the two-point circular functions pt and tp we have

$$(4.8) \qquad \mathsf{pt}(s,\sigma) = \mathsf{tp}(\sigma,s) = \frac{\mathsf{pp}(s,\sigma)}{|\sin\theta_{s\sigma'}|}, \quad (s \neq \sigma)$$

where $\theta_{s\sigma'}$ is the angle between $\boldsymbol{q}(s) - \boldsymbol{q}(\sigma)$ and the tangent vector to $\mathcal{C}$ at $\boldsymbol{q}(\sigma)$. When $\sin\theta_{s\sigma'} = 0$ we set $\mathsf{pt}(s,\sigma) = \infty$. Note that (4.8) is the limit of (4.3) as the triangle closes.

For the two-point spherical function tt we find

$$(4.9) \qquad \mathsf{tt}^2(s,\sigma) = \mathsf{pp}^2(s,\sigma) \, \frac{1 - \big(\boldsymbol{t}(\sigma) \cdot \boldsymbol{R}(e)\boldsymbol{t}(s)\big)^2}{|\boldsymbol{t}(s) \times \boldsymbol{t}(\sigma) \cdot e|^2}, \quad (s \neq \sigma)$$

where $\boldsymbol{t}(s) \times \boldsymbol{t}(\sigma) \cdot e$ is the standard scalar triple product,

$$(4.10) \qquad e = \frac{\boldsymbol{q}(s) - \boldsymbol{q}(\sigma)}{|\boldsymbol{q}(s) - \boldsymbol{q}(\sigma)|}$$

is the unit vector along the chord, and

$$(4.11) \qquad \boldsymbol{R}(e) = [2e \otimes e - \boldsymbol{I}]$$

with $e \otimes e$ being the usual vector outer product so that $\boldsymbol{R}(e)$ is the (symmetric) proper rotation matrix that maps the curve tangent $\boldsymbol{t}(\sigma)$ into the (compatibly oriented) tangent $\boldsymbol{t}^\star(s,\sigma)$ at $\boldsymbol{q}(s)$ of the circle $\mathcal{C}(\sigma,\sigma,s)$ (which was defined as the circle with tangent $\boldsymbol{t}(\sigma)$ at $\boldsymbol{q}(\sigma)$ passing through the point $\boldsymbol{q}(s)$). Formula (4.9) is valid whenever the two tangents and the chord associated with (s,σ) are linearly independent. In the case when they are linearly dependent we set $\mathsf{tt}(s,\sigma) = \infty$, unless they are co-circular in the sense that $\mathcal{C}(s,\sigma,\sigma) = \mathcal{C}(s,s,\sigma)$, in which case we set $\mathsf{tt}(s,\sigma) = \mathsf{pt}(s,\sigma) = \mathsf{tp}(s,\sigma)$.

As $\boldsymbol{t}(s)$ and $\boldsymbol{t}(\sigma)$ are unit vectors and $\boldsymbol{R}(e)$ is a rotation matrix, $\boldsymbol{t}(\sigma) \cdot \boldsymbol{R}(e)\boldsymbol{t}(s)$ is the cosine of the angle $\psi(s,\sigma)$ between the unit vectors $\boldsymbol{t}(s)$ and $\boldsymbol{t}^\star(s,\sigma)$ and we may rewrite (4.9) as

$$(4.12) \qquad \mathsf{tt}(s,\sigma) = \mathsf{pp}(s,\sigma) \, \frac{|\sin\psi(s,\sigma)|}{|\boldsymbol{t}(s) \times \boldsymbol{t}(\sigma) \cdot e|}, \quad (s \neq \sigma).$$

The angle ψ has previously been considered in various knot energies [13, p. 318], [16, p. 294].

Formulæ for the two-point spherical functions cp and pc are also available. In particular, let (α, β, γ) be the coordinates of $\boldsymbol{q}(\sigma)$ with respect to the Frenet frame at $\boldsymbol{q}(s)$ in the sense that

$$(4.13) \qquad \boldsymbol{q}(\sigma) = \boldsymbol{q}(s) + \alpha \boldsymbol{t}(s) + \beta \boldsymbol{n}(s) + \gamma \boldsymbol{b}(s).$$

Then we find

$$(4.14) \qquad \mathsf{cp}(s, \sigma) = \mathsf{pc}(\sigma, s) = \sqrt{\rho^2(s) + \frac{[\alpha^2 + \beta^2 + \gamma^2 - 2\beta\rho(s)]^2}{4\gamma^2}}, \quad (s \neq \sigma).$$

This formula is valid whenever $\gamma \neq 0$, that is, $\boldsymbol{q}(\sigma) \notin \mathcal{P}(s)$. When $\boldsymbol{q}(\sigma) \in \mathcal{P}(s)$ we set $\mathsf{cp}(s, \sigma) = \infty$, unless $\boldsymbol{q}(\sigma) \in \mathcal{C}(s)$ in which case we set $\mathsf{cp}(s, \sigma) = \rho(s)$.

For points s at which $\tau(s) \neq 0$, formula (4.14) suggests the definition

$$(4.15) \qquad \mathsf{cp}(s, s) = \lim_{\sigma \to s} \mathsf{cp}(s, \sigma) = \rho_{os}(s).$$

However, just as in Remarks 3.1, the most appropriate definition for $\mathsf{cp}(s, s)$ at points with $\tau(s) = 0$ is unclear.

4.4. Multi-point radius inequalities. The functions pp, ppp and pppp satisfy the basic inequalities:

$$(4.16) \qquad 0 \leq \mathsf{pp}(s, t) \leq \mathsf{ppp}(s, t, \sigma) \leq \mathsf{pppp}(s, t, \sigma, \tau), \quad (s, t, \sigma, \tau \quad \text{distinct}),$$

which follow from the facts that the half-length of any chord on a circle is bounded by the circle radius, and the radius of any circle on a sphere is bounded by the sphere radius.

By considering various coalescent limits in (4.16) we arrive at inequalities involving the associated limit functions. For example, for the limit functions with three-point arguments we find

$$(4.17) \qquad \mathsf{ppp}(s, t, \sigma) \leq \begin{cases} \mathsf{ppt}(s, t, \sigma) \\ \mathsf{ptp}(s, t, \sigma) \\ \mathsf{tpp}(s, t, \sigma) \end{cases} \quad (s, t, \sigma \quad \text{distinct}),$$

and for the limit functions with two-point arguments we find

$$(4.18) \qquad \mathsf{pp}(s, t) \leq \begin{cases} \mathsf{pt}(s, t) & \leq \begin{cases} \mathsf{pc}(s, t) \\ \mathsf{tt}(s, t) \end{cases} \\ \mathsf{tp}(s, t) & \leq \begin{cases} \mathsf{tt}(s, t) \\ \mathsf{cp}(s, t) \end{cases} \end{cases} \quad (s, t \quad \text{distinct}),$$

where in (4.17) and (4.18) it is to be understood that the braces indicate alternatives.

There exist curves Γ with pairs of points (s, t) such that all of the inequalities (4.18) are sharp. Contrariwise, pairs of points of closest (or stationary) approach, i.e. pairs of distinct points $\boldsymbol{q}(s)$ and $\boldsymbol{q}(t)$ and associated curve tangents $\boldsymbol{t}(s)$ and $\boldsymbol{t}(t)$ satisfying

$$(4.19) \qquad \boldsymbol{t}(s) \cdot (\boldsymbol{q}(s) - \boldsymbol{q}(t)) = \boldsymbol{t}(t) \cdot (\boldsymbol{q}(s) - \boldsymbol{q}(t)) = 0,$$

are very special because at such pairs we always have equality between four of the two-point radius functions

$$(4.20) \qquad \mathsf{pp}(s, t) = \mathsf{pt}(s, t) = \mathsf{tp}(s, t) = \mathsf{tt}(s, t).$$

5. Global radius of curvature functions

To any simple curve Γ and multi-point radius function we may associate a global radius of curvature function defined by minimizing over all but the first argument, namely

$$
\begin{aligned}
\rho_{\mathsf{pppp}}(s) &= \inf_{t,\sigma,\tau} \mathsf{pppp}(s,t,\sigma,\tau) & (s,t,\sigma,\tau \quad \text{distinct}) \\
\rho_{\mathsf{ppp}}(s) &= \inf_{t,\sigma} \mathsf{ppp}(s,t,\sigma) & (s,t,\sigma \quad \text{distinct}) \\
\rho_{\mathsf{pt}}(s) &= \inf_t \mathsf{pt}(s,t) & (s,t \quad \text{distinct}) \\
&\;\;\vdots \\
\rho_{\mathsf{pp}}(s) &= \inf_t \mathsf{pp}(s,t) = 0 & (s,t \quad \text{distinct}).
\end{aligned}
$$

These functions may be viewed as generalizations of the standard local radius of curvature functions $\rho(s)$ and $\rho_{\mathrm{os}}(s)$. Here we study various properties of these global radius of curvature functions, and discuss the non-local information that they contain about Γ.

5.1. Radius of curvature inequalities. The radius of curvature functions are nested at each point $\boldsymbol{q}(s)$. In particular, for the circular radius of curvature functions we have

$$
(5.1) \qquad \rho \geq \left\{ \begin{array}{c} \rho_{\mathsf{tp}} \\ \rho_{\mathsf{pt}} \end{array} \right\} \geq \rho_{\mathsf{ppp}}.
$$

These inequalities follow from the observation that any circle which achieves any radius function on the left is a competitor (or limit of competitors) for any function on the right. Similarly, the spherical radius functions satisfy

$$
(5.2) \qquad \rho_{\mathrm{os}} \geq \left\{ \begin{array}{c} \left. \begin{array}{c} \rho_{\mathsf{pc}} \\ \rho_{\mathsf{tt}} \\ \rho_{\mathsf{cp}} \end{array} \right\} \geq \rho_{\mathsf{ppt}} = \rho_{\mathsf{ptp}} \\[1em] \left. \begin{array}{c} \rho_{\mathsf{tt}} \\ \rho_{\mathsf{cp}} \end{array} \right\} \geq \rho_{\mathsf{tpp}} \end{array} \right\} \geq \rho_{\mathsf{pppp}}.
$$

5.2. Distinct radius of curvature functions. When Γ is a simple, closed or infinite, curve we find various equalities between the circular and spherical radius of curvature functions. In particular, at each point $\boldsymbol{q}(s)$ we have

$$
(5.3) \qquad \rho_{\mathsf{pt}} = \rho_{\mathsf{ppp}} = \rho_{\mathsf{ptp}} = \rho_{\mathsf{ppt}} = \rho_{\mathsf{pppp}},
$$

$$
(5.4) \qquad \rho_{\mathsf{tt}} = \rho_{\mathsf{tpp}} = \rho_{\mathsf{tp}},
$$

and

$$
(5.5) \qquad \rho = \rho_{\mathsf{cp}}^{\star}.
$$

The first equality in (5.3) was derived in [**8**, p. 4770], and the further relations in (5.3) and (5.4) are implied by similar arguments. The central idea in all of the demonstrations is that a sphere realizing the minimum in the definition of a global radius of curvature function at the point s, cannot have only zero-order intersections at distinct points, for otherwise the sphere could be shrunk, while retaining the same number of intersections with the curve Γ, and the same order of contact at s, contradicting optimality.

The equality (5.5) is of a different character as it relates the entirely local object ρ with a global radius of curvature. Moreover here the asterisk indicates that the

equality only holds at points at which either $\kappa'(s) \neq 0$ or $\tau(s) \neq 0$. At points where $\kappa'(s) = \tau(s) = 0$ the very definition of $\rho_{\mathsf{cp}}(s)$ is unclear. For the demonstration of the generic case, note first that $\mathsf{cp}(s, \sigma) \geq \rho(s)$ because any sphere with second-order contact at s contains the osculating circle at s. Thus $\rho_{\mathsf{cp}}(s) \geq \rho(s)$. If $\kappa'(s) \neq 0$ the opposite inequality (and therefore equality) follows from the Taylor expansion (3.5). In particular, the curve locally crosses the osculating circumsphere $\mathbb{S}^c$ near $\boldsymbol{q}(s)$. Since the curve Γ is simple and has no end-points (it is closed or infinite) it must re-cross the sphere $\mathbb{S}^c$ at some distinct point $\boldsymbol{q}(\sigma)$, which leads to the conclusion that $\mathsf{cp}(s, \sigma) = \rho(s)$, so that $\rho_{\mathsf{cp}}(s) \leq \rho(s)$. When $\kappa'(s) = 0$ but $\tau(s) \neq 0$, we have by (4.15) and (3.4) that $\lim_{\sigma \to s} \mathsf{cp}(s, \sigma) = \rho_{\mathsf{os}}(s) = \rho(s)$, so $\rho_{\mathsf{cp}}(s) \leq \rho(s)$.

Thus for simple, closed or infinite, curves we have the seven equalities (5.3)–(5.5) which imply that of the possible twelve radius of curvature functions there are only five distinct ones. The functions $\{\rho_{\mathsf{pt}}, \rho_{\mathsf{tt}}, \rho_{\mathsf{pc}}, \rho, \rho_{\mathsf{os}}\}$ can be taken as an independent set. Combining inequalities (5.1) and (5.2) with equalities (5.3)–(5.5), implies that these five functions are nested in the sense

$$(5.6) \qquad \rho_{\mathsf{os}} \geq \left\{ \begin{array}{c} \rho \geq \rho_{\mathsf{tt}} \\ \rho_{\mathsf{pc}} \end{array} \right\} \geq \rho_{\mathsf{pt}} \geq 0.$$

We can then address the question of identifying special points along the curve at which equalities can occur between some or all of the five independent curvature functions. For example, equalities between the global radius of curvature functions ρ_{pt} and ρ_{tt} can arise at points of closest approach as described in Section 4.4. Equality between local and global radius of curvature functions can occur only at certain special points along Γ. Specifically, for a simple, closed or infinite, curve, equality between ρ_{pt} and ρ can occur only at extremal points of the local curvature κ in the sense that

$$(5.7) \qquad \kappa \neq 0 \quad \text{and} \quad \rho_{\mathsf{pt}} = \rho \quad \Rightarrow \quad \kappa' = 0 \quad \text{and} \quad \kappa'' \leq \kappa \tau^2.$$

Notice that these extremal points must be maxima (to second order) of the local curvature whenever the torsion is zero, as would be the case for planar curves. This result follows from the Taylor expansion (3.5). The proof is by contradiction: suppose that $\rho_{\mathsf{pt}}(s) = \rho(s)$ and that $\kappa'(s) \neq 0$. Then Γ locally pierces the osculating circumsphere $\mathbb{S}^c(s)$ of radius $\rho(s)$. Since Γ is simple and has no end-points (it is closed or infinite) it must re-cross $\mathbb{S}^c(s)$ at a distinct point $\boldsymbol{q}(\sigma)$. Then we can shrink $\mathbb{S}^c(s)$ to find a sphere of smaller radius than $\rho(s)$ that is tangent at $\boldsymbol{q}(s)$ and which intersects Γ near $\boldsymbol{q}(\sigma)$. By considering circles on this sphere we find $\rho_{\mathsf{tt}}(s) = \rho_{\mathsf{tp}}(s) < \rho(s) = \rho_{\mathsf{pt}}(s)$, a contradiction of (5.6). Thus $\kappa'(s) = 0$ is a necessary condition. If the second condition $\kappa'' \leq \kappa \tau^2$ were violated the expansion (3.5) reveals that the curve would locally lie inside the osculating circumsphere $\mathbb{S}^c(s)$. A similar shrinking argument would then lead to a contradiction as before.

Notice that if $\kappa \neq 0$ and $\rho_{\mathsf{pt}} = \rho$, then all the circular radius of curvature functions (both local and global) must be equal by virtue of (5.1) and (5.3). If moreover $\tau \neq 0$, then all the radius of curvature functions introduced thus far (both circular and spherical, local and global) must be equal by virtue of (3.4), (5.2), (5.3) and (5.4).

6. Thickness of closed or infinite curves

Let Γ be a simple, closed or infinite, curve. Then to each of the five distinct radius of curvature functions $\{\rho_{\mathsf{pt}}, \rho_{\mathsf{tt}}, \rho_{\mathsf{pc}}, \rho, \rho_{\mathsf{os}}\}$ we may associate a functional (or number) corresponding to its infimum:

$$\Delta_{\mathsf{pt}}[\Gamma] = \inf_s \rho_{\mathsf{pt}}(s), \quad \Delta_{\mathsf{tt}}[\Gamma] = \inf_s \rho_{\mathsf{tt}}(s),$$

and so on. Arguments involving properties of minimizing circles and spheres show that

(6.1) $$\Delta_{\rho_{\mathsf{os}}}[\Gamma] \geq \Delta_{\mathsf{pc}}[\Gamma] = \Delta_\rho[\Gamma] \geq \Delta_{\mathsf{tt}}[\Gamma] = \Delta_{\mathsf{pt}}[\Gamma].$$

Thus for simple, closed or infinite, curves we have only three distinct functionals of this type, namely Δ_{pt}, Δ_ρ and $\Delta_{\rho_{\mathsf{os}}}$. The number Δ_ρ is just the minimal value of the local osculating circle radius of curvature ρ along the curve, while $\Delta_{\rho_{\mathsf{os}}}$ is the minimal value of the local osculating sphere radius of curvature ρ_{os}. For smooth curves with non-vanishing torsion, formula (3.4) reveals that $\rho_{\mathsf{os}}(s) = \rho(s)$, whenever $\rho'(s) = 0$. Consequently $\Delta_{\rho_{\mathsf{os}}}[\Gamma] = \Delta_\rho[\Gamma]$ for such curves. However in general the two numbers are different, as can be seen, for example, by consideration of smooth, non-circular closed curves lying on a given sphere.

The number Δ_{pt} is more interesting. It was first introduced in [8] within the context of the study of ideal or tight knots, where it was shown that $\Delta_{\mathsf{pt}} = \Delta_{\mathsf{ppp}}$ gives an explicit characterization of the normal injectivity radius Inj or thickness of the curve Γ. With the last equality in (6.1), we see that the thickness could also be computed via a numerical evaluation of $\Delta_{\mathsf{tt}}[\Gamma]$. Consideration of smooth, simple curves that are close to a figure eight, demonstrates that strict inequality between Δ_ρ and Δ_{pt} is possible.

Remark 6.1 The last equality of (6.1) relies on the fact that a simple, closed or infinite, curve has no end-point. In particular, this equality is violated for the curve with end-points that is sketched in Figure 3. Here $\rho_{\mathsf{tt}}(s) = R = 2r > r = \rho_{\mathsf{pt}}(s)$. And, by taking r as small as necessary, we see that $\Delta_{\mathsf{tt}}[\Gamma] = \rho_{\mathsf{tt}}(s)$ while $\Delta_{\mathsf{pt}}[\Gamma] = \rho_{\mathsf{pt}}(s)$, so that the last equality in (6.1) fails. Moreover $\rho_{\mathsf{tp}}(\sigma) = r < \rho_{\mathsf{tt}}(\sigma)$, which shows that the identity (5.4) can also fail in the presence of end-points.
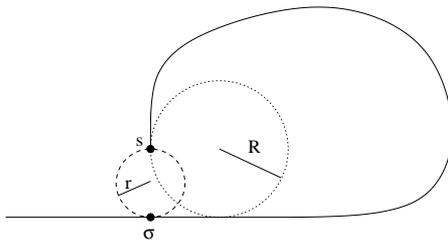

FIGURE 3. A curve Γ that illustrates the effects of end-points on global radius of curvature functions and curve thickness. The curve is drawn such that $\Delta_{\mathsf{tt}}[\Gamma] = \rho_{\mathsf{tt}}(s) = R = 2r > r = \rho_{\mathsf{pt}}(s) = \Delta_{\mathsf{pt}}[\Gamma]$.

7. Examples

7.1. Ellipses. Here we illustrate various properties of the standard local radius of curvature function ρ, and the global radius of curvature functions ρ_{pt} and ρ_{tt} for the case when Γ is an ellipse.

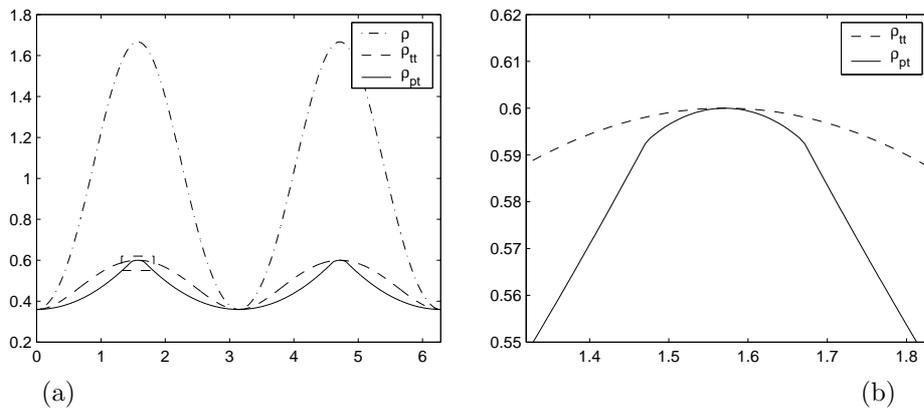
(a)   (b)

FIGURE 4. Plots of local and global radius of curvature functions for an ellipse with principal axes of length 1.0 and 0.6: (a) ρ, ρ_{pt} and ρ_{tt} versus the polar angular coordinate around the ellipse (with $\theta = 0$ corresponding to a vertex of minimal radius of curvature), (b) magnified view of ρ_{pt} and ρ_{tt} near their common maxima at $\theta = \pi/2$ (corresponding to the inset of part a).

Figure 4 shows plots of ρ, ρ_{pt} and ρ_{tt} along a particular ellipse. Nestedness between all three functions is in agreement with (5.6). Moreover, equality between all three functions occurs only at local minima of ρ (equivalently, local maxima of κ), which is in accordance with (5.7) in the case of zero torsion. The two global radius of curvature functions also coincide at the ends of the minor axes, which are a pair of points of stationary approach as defined in (4.19). While ρ_{tt} is smooth, ρ_{pt} has corners near each of its local maxima. As discussed below, these corners are associated with a discontinuity in the family of minimizing circles for ρ_{pt}.

Figure 5 illustrates various properties of the osculating and minimizing circles associated with the functions ρ, ρ_{pt} and ρ_{tt} on an ellipse. Panel (a) shows the locus of centers of all osculating circles, and the loci of the centers of all minimizing circles associated with ρ_{tt} and ρ_{pt}. The osculating and ρ_{pt} loci actually coincide on the two arrow-head portions, which fact is explained later. Panel (b) illustrates the classic (but apparently not widely-known) result that for planar curves the osculating circles are nested between extremal points, or vertices, of the local radius of curvature ρ (see, e.g. [**11**, Theorem 3-12, p. 48], [**21**, p. 403]). In panel (c) we plot the minimizing circles associated with ρ_{tt} for various points along the ellipse. These circles are actually osculating circles at the two local minima of ρ, i.e. at the left and right end-points of the line segment, but minimizing circles with centers at interior points are instead doubly tangent at distinct points of the ellipse. Panels (d)–(f) illustrate the minimizing circles for ρ_{pt}. Panel (d) depicts the continuous, nested, family of minimizing circles with centers on the arrow-head portion of the locus of centers. The minimizing circles are non-unique at the point illustrated in panel (e),
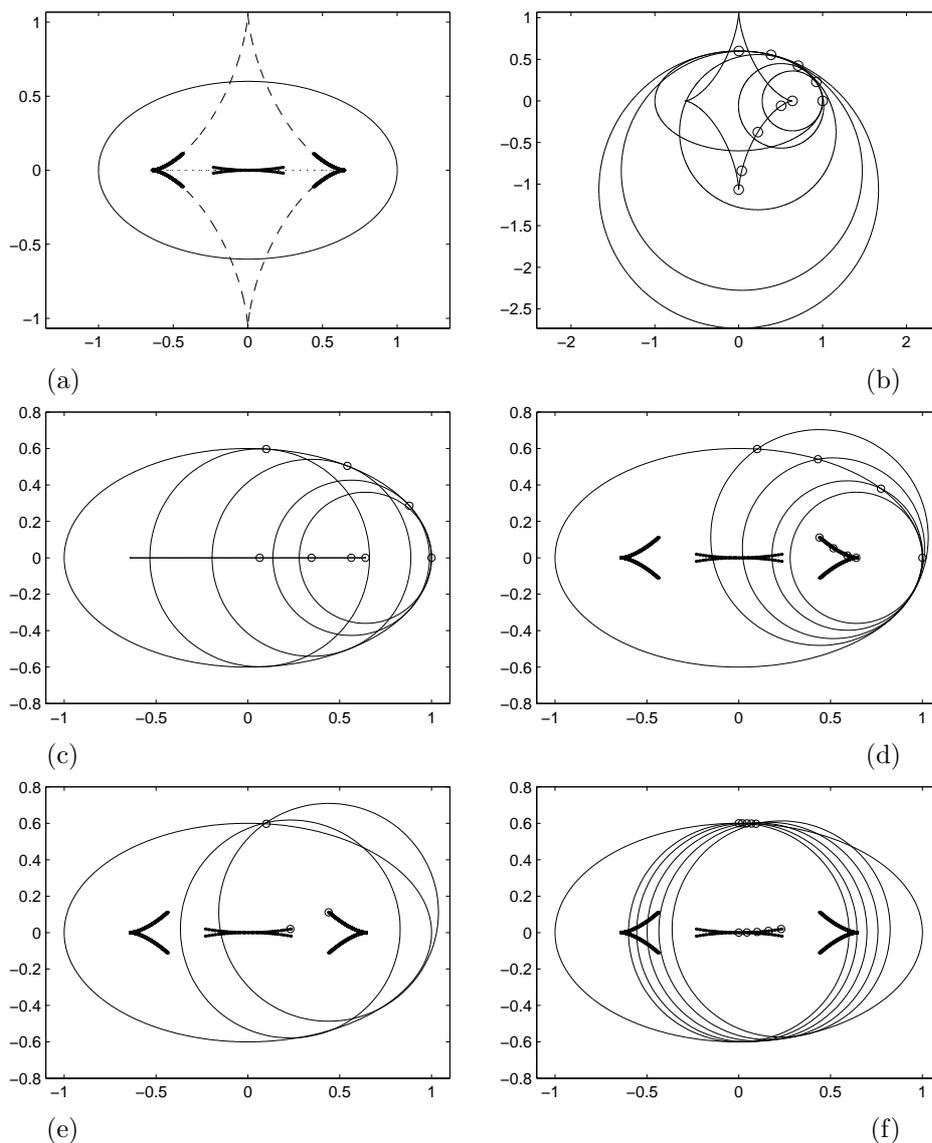
FIGURE 5. Osculating circles associated with ρ and minimizing circles associated with ρ_{tt} and ρ_{pt} for an ellipse: (a) three loci of the centers of i) the osculating circles (diamond-shaped curve drawn in dashes), ii) the minimizing circles realizing ρ_{tt} (horizontal line segment drawn in small dots), and iii) the minimizing circles realizing ρ_{pt} (dark curve with discontinuities), (b) various osculating circles with centers and tangency points marked in open dots, (c) various minimizing circles for ρ_{tt}, (d)-(f) minimizing circles for ρ_{pt} with (d) centers on the arrow-head portion of the locus of centers, (e) two minimizing circles with the same radius, but different centers lying on either side of the discontinuity in the locus, and (f) non-nested minimizing circles with centers on the central portion of the locus.

and then the (non-nested) family of minimizing circles smoothly evolves, as shown in panel (f). It is this transition between two smooth families of minimizing circles that explains the corner in the graph of $\rho_{\mathsf{pt}}(s)$ that can be seen in Figure 4 (b).

It remains to discuss the nestedness of the circles appearing in Figure 5 (d). The numerics indicate that the minimizing circle at s has zeroth-order contact with the ellipse at s. The minimizing circle for ρ_{pt} must, by definition, have a first-order intersection or tangency to the ellipse at some point σ. For all but one of the circles in part (d) the point σ is distinct from s, and, moreover, there is no other intersection between each minimizing circle and the ellipse. By a crossing argument this means that the order of contact between the ellipse and circle (i.e. two closed planar curves) at σ must be at least of second-order. Thus the circle realizing the minimum in $\rho_{\mathsf{pt}}(s)$ is in fact the osculating circle to the ellipse at σ, so that $\rho_{\mathsf{pt}}(s) = \rho(\sigma)$. Therefore the loci of centers of minimizing circles for ρ_{pt} and the osculating circles coincide locally, and local nestedness follows from the known nestedness of osculating circles.

7.2. Helices. Helices are perhaps the simplest non-planar curves. Because helices are uniform, any radius of curvature function must be constant. However for helices it is interesting to consider how the various radius of curvature functions are realized as minima of the linear pp, circular $\{\mathsf{pt}, \mathsf{tp}\}$ and spherical $\{\mathsf{cp}, \mathsf{pc}, \mathsf{tt}\}$ two-point radius functions. Precisely because helices are uniform, it suffices to fix an arbitrary point s on the helix and to examine how the two-point radius functions vary with the second argument σ. It can be shown that helices possess a discrete symmetry which implies $\mathsf{pt}(s, \sigma) = \mathsf{tp}(s, \sigma)$ and $\mathsf{pc}(s, \sigma) = \mathsf{cp}(s, \sigma)$. Accordingly, we consider only one independent circular function pt and two independent spherical functions $\{\mathsf{cp}, \mathsf{tt}\}$.

Figures 6 (a,b) show plots of pp, pt, cp and tt as functions of the difference in arclength $\eta = \sigma - s$ for a helix of pitch 1.2. (In all our examples the helices are scaled to have radius one.) Nestedness between the linear, circular and spherical functions is in agreement with (4.18), as is the non-nestedness of the spherical functions cp and tt. (For helices the function tt tends to infinity near distinct points (s, σ) where the associated tangents are parallel.) Notice that the circular function pt and the spherical function tt enjoy the same global minimal value, as asserted by the last equality in (6.1), that the global minimum of cp is strictly larger (i.e. the second inequality in (6.1) is actually strict for this curve), and that, trivially, the global minimum of pp is zero.

Figure 6 (c) illustrates how the minima of various two-point functions depend on the helix pitch. For the helices with pitches 4 and 2.8, $\mathsf{pt}(s, \sigma)$ achieves its global minimum at $\eta = \sigma - s = 0$. For pitch 4 the global minimum is the only local minimum, whereas for pitch 2.8 there are two other local minima. The fact that the global minimum is achieved at $\eta = 0$ implies the thickness equality $\Delta_\rho[\Gamma] = \Delta_{\mathsf{pt}}[\Gamma]$ since the limit function $\mathsf{pt}(s, s)$ is just the standard local radius of curvature $\rho(s)$. For the helix with pitch 1.5, pt achieves its global minimum for $\eta \neq 0$; moreover, this minimum value is strictly less than its value at the local minimum $\eta = 0$. Thus for pitch 1.5 we have the strict inequality $\Delta_\rho[\Gamma] > \Delta_{\mathsf{pt}}[\Gamma]$, and the thickness is achieved by a circle (or sphere) that intersects the helix at two distinct points. For the helix with pitch $2.5126\ldots$, pt achieves its global minimum both at $\eta = 0$ and at $\eta \neq 0$. Thus the thickness of a helix with this critical pitch is determined simultaneous by local and global properties of the curve. Maritan *et al* [**15**] originally identified this
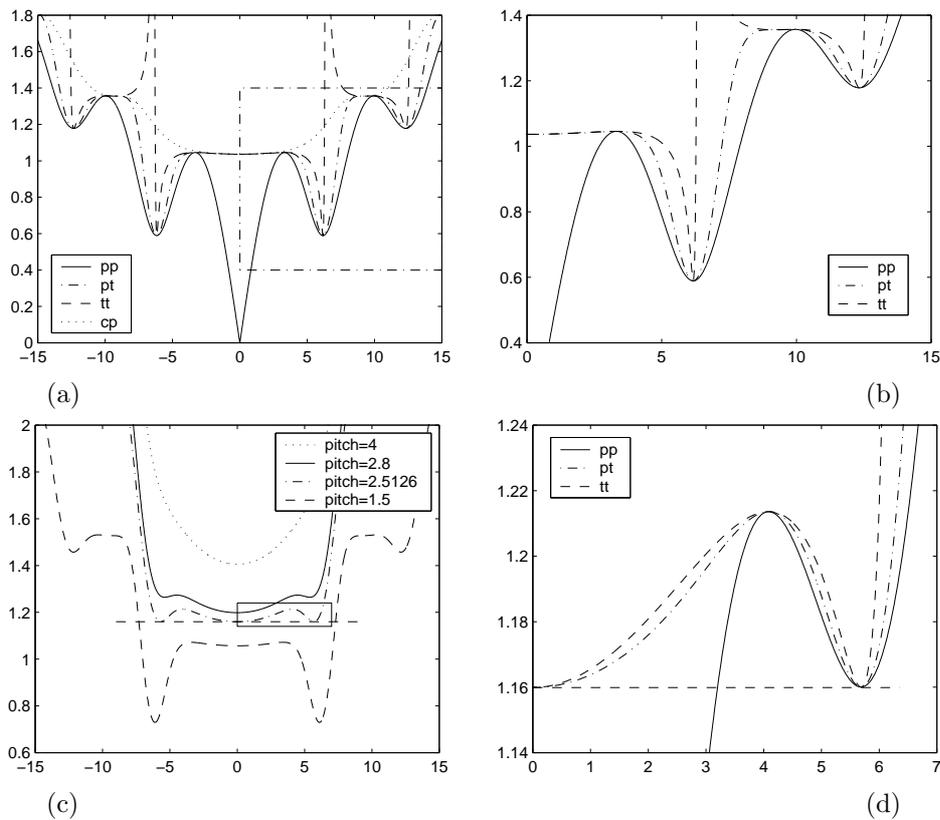
FIGURE 6. Plots of linear, circular, and spherical, two-point radius functions for helices: (a) pp, pt, cp, and tt versus $\eta = \sigma - s$ for a helix of pitch 1.2, (b) magnification of the inset shown in part (a), (c) plots of the single function pt for four helices with different pitches 1.5, 2.5126, 2.8 and 4. The horizontal line segment emphasizes the equality of the three local minima for the critical pitch 2.5126 of Maritan *et al* [**15**], (d) plots of the three functions pp, pt and tt on the single critical-pitch helix within the inset indicated in part (c).

critical pitch in their work on the optimal packing of filaments. They also observed that many crystal structures of helical proteins have the same critical pitch. The critical helix is further illustrated in Figure 7.

In all of our discussions we are by no means restricted to consider only connected curves. Curves made up of multiple helices with a common axis, diameter and pitch, remain uniform (cf. Figure 8), and therefore have constant radius of curvature functions. Accordingly, just as for single helices, we can plot linear, circular and spherical two-point radius functions for various double helices. In Figure 9, panels (a) and (c) show the symmetric case of diametrically opposed strands (an offset angle of π), and in (b) and (d) an unsymmetric case in which the strands are offset by an angle of $\frac{2}{3}\pi$. Panels (a) and (b) each plot the functions pp, pt and tt for one double-helical structure (pitch = 2.5126), while panels (c) and (d) plot the single
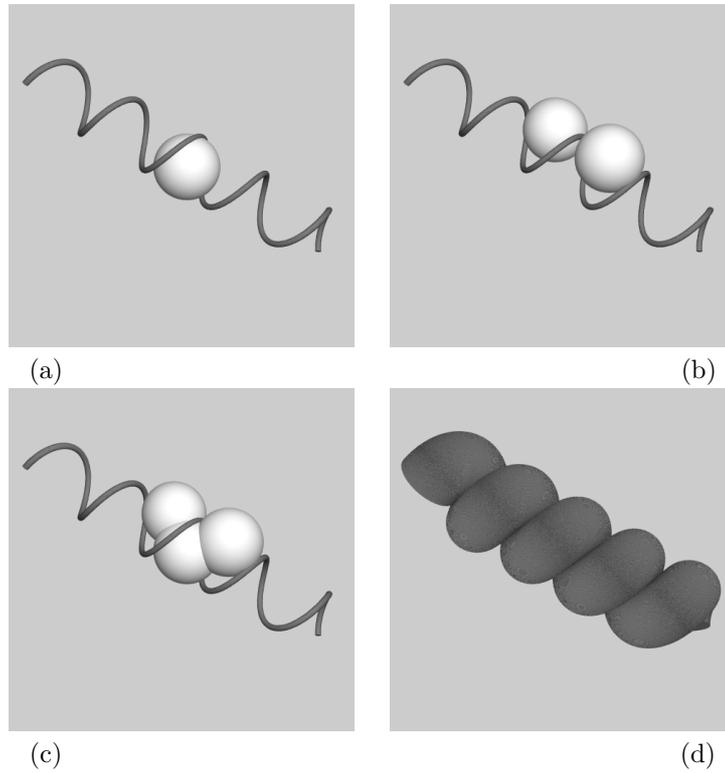
FIGURE 7. Visualization of the pitch 2.5126 critical single helix: (a) the local osculating circumsphere (which is also the osculating sphere) associated with ρ, (b) two doubly-tangent spheres of radius ρ that achieve ρ_{pt}, (c) superposition of the local and global spheres, (d) the tube formed as the envelope of all spheres with radius equal to the thickness $\Delta_{\mathsf{pt}}[\Gamma]$ that are centered on the helix.
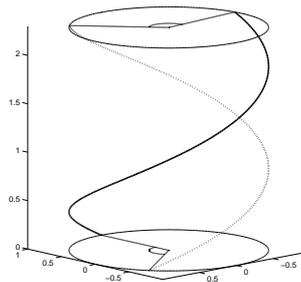

FIGURE 8. Structure formed by two helices with common axis, diameter and pitch, and constant offset angle (here 0.7π).

function pt for a range of pitches. It can be shown that in all cases, $\Delta_{\mathsf{pt}}[\Gamma] = \Delta_{\mathsf{tt}}[\Gamma]$ is achieved by a circle that intersects both strands, or, equivalently, by a sphere that sits between the two strands with tangencies at either side. Panel (c) shows
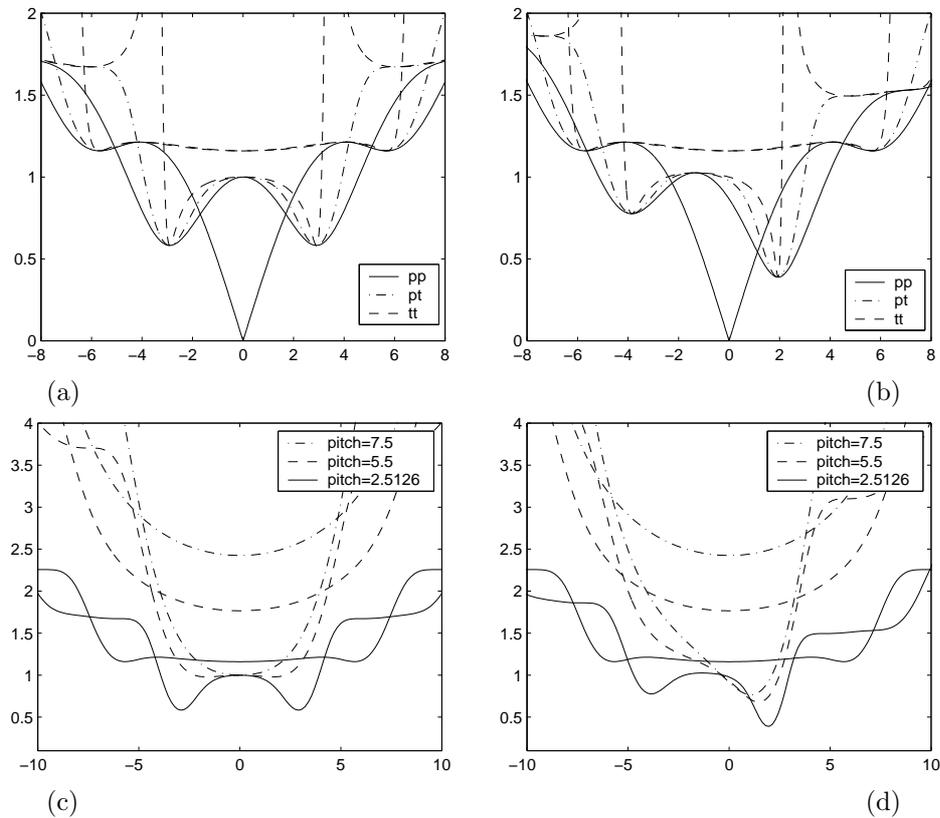
FIGURE 9. Plots of linear, circular, and spherical, two-point radius functions on double helices. The arclength parameter $\eta = \sigma - s$ now assumes all real values twice, once corresponding to pairs of points on the same strand, and once with the pair on opposite strands (with phasing chosen such that $\eta = 0$ corresponds to points on opposite strands that lie in the same orthogonal cross-section of the double helical structure). Accordingly, the plot of each function generates two curves (one for each strand): (a) pp, pt, and tt for pitch 2.5126, and offset angle π (i.e. the diametrically opposed double helix), (b) same as (a) but with offset angle $\frac{2}{3}\pi$, (c) pt for three different pitches, all with offset angle π, (d) same as (c), but with offset angle $\frac{2}{3}\pi$.

that as the pitch is decreased, there is a critical value at which a global minimum of pt, achieved across the diameter of the helical structure, splits into two global minima, achieved by asymmetric leading and trailing spheres (and a symmetric local maximum). Unlike the single helix, this transition, or bifurcation, for the double helix is local and for this reason it is easy to calculate analytically that the critical pitch is exactly 2π. In [19] it was observed that this critical pitch value corresponds to the standard parameters for the B-form DNA double helix. For asymmetrically offset double helices, as shown in panel (d), there is a critical pitch

below which there are multiple local minima of the function pt. However for all pitch values there is always a unique global minimum that varies smoothly.

References

[1] Berger, M., *Geometry I*, Springer, Berlin Heidelberg (1987).

[2] Blumenthal, L.M., *Theory and applications of distance geometry*, Second Edition, Chelsea, New York (1970).

[3] Buck, G. and Simon, J., *Energy and length of knots*, in Lectures at Knots96, ed. Suzuki, S., World Scientific Publishing, Singapore (1997) 219–234.

[4] Cantarella, J., Kusner, R. and Sullivan, J.M., *On the minimum ropelength of knots and links*, Inventiones Math, to appear.

[5] Coxeter, H.S.M., *Introduction to Geometry*, Second Edition, Wiley, New York (1969).

[6] Do Carmo, M., *Riemannian Geometry*, Birkäuser, Boston, Basel, Berlin (1992).

[7] Gonzalez, O. and de la Llave, R., *Existence of ideal knots*, Journal of Knot Theory and its Ramifications, to appear.

[8] Gonzalez, O. and Maddocks, J.H., *Global curvature, thickness and the ideal shapes of knots*, Proc. Natl. Acad. Sci. USA **96** (1999) 4769–4773.

[9] Gonzalez, O., Maddocks, J.H., Schuricht, F. and von der Mosel, H., *Global curvature and self-contact of nonlinearly elastic curves and rods*, Calculus of Variations, **14** (2002) 29–68 (DOI 10.1007/s005260100089, April 2001).

[10] Graustein, W.C., *Differential Geometry*, Dover Publications, New York (1966).

[11] Guggenheimer, H.W., *Differential Geometry*, Dover, New York (1977).

[12] Katritch, V., Bednar, J., Michoud, D., Scharein, R.G., Dubochet, J. and Stasiak, A., *Geometry and physics of knots*, Nature **384** (1996) 142–145.

[13] Kusner, R., and Sullivan, J.M., *Möbius-Invariant Knot Energies.* Chpt. 17 of [**18**].

[14] Litherland, R.A., Simon, J., Durumeric, O. and Rawdon, E., *Thickness of knots*, Topology and its Applications **91** (1999) 233–244.

[15] Maritan, A., Micheletti, C., Trovato, A. and Banavar, J.R., *Optimal shapes of compact strings*, Nature **406** (2000) 287–290.

[16] O'Hara, J., *Energy of Knots*, Chpt. 16 of [**18**].

[17] Schuricht, T., von der Mosel, H., *Global curvature for rectifiable loops*, Mathematische Zeitschrift, to appear.

[18] Stasiak, A., Katritch, V. and Kauffman, L.H., Editors, *Ideal Knots*, World Scientific Publishing, Singapore (1998).

[19] Stasiak, A. and Maddocks, J.H., *Best packing in proteins and DNA*, Nature **406** (2000) 251–253.

[20] Struik, D.J., *Lectures on Classical Differential Geometry*, Second Edition, Dover, New York (1988).

[21] Tait, P. G., *Scientific papers*, Vol. II, Cambridge University Press, (1900).

Department of Mathematics, The University of Texas, Austin, TX 78712
E-mail address: og@math.utexas.edu

Bernoulli Institute, Swiss Federal Institute of Technology, Lausanne , CH-1015, Switzerland
E-mail address: john.maddocks@epfl.ch

Bernoulli Institute, Swiss Federal Institute of Technology, Lausanne , CH-1015, Switzerland
E-mail address: jana.smutny@epfl.ch